Influence of the cubic anisotropy constants on the hysteresis loops of single-domain particles: A Monte Carlo study

J. García-Otero
Departamento de Física Aplicada, Facultade de Físicas, Universidade de Santiago de Compostela, Campus Sur s/n, E-15706 Santiago de Compostela, Spain

M. Porto
Institut für Theoretische Physik III, Justus-Liebig-Universität Giessen, Heinrich-Buff-Ring 16, D-35392 Giessen, Germany

J. Rivas[a)]
Departamento de Física Aplicada, Facultade de Físicas, Universidade de Santiago de Compostela, Campus Sur s/n, E-15706 Santiago de Compostela, Spain

A. Bunde
Institut für Theoretische Physik III, Justus-Liebig-Universität Giessen, Heinrich-Buff-Ring 16, D-35392 Giessen, Germany

(Received 8 September 1998; accepted for publication 13 November 1998)

The influence of the first and second cubic anisotropy constants on the hysteresis loops of noninteracting single-domain magnetic particles is studied by Monte Carlo simulation, which turns out to be a very powerful method for studying simple magnetic models. Both signs in the anisotropy constants are taken into account. Relevant properties such as coercivity and remanence are studied as a function of temperature when the second anisotropy constant is negligible. The influence of the second term of the anisotropy energy is studied in detail for $T=0$ K. It is concluded that this term has a big influence on the static magnetic behavior when the first anisotropy constant is negative. © *1999 American Institute of Physics.* [S0021-8979(99)07004-8]

I. INTRODUCTION

The study of fine magnetic particles is nowadays one of the most important challenges of modern technology because it provides new opportunities for a better understanding of magnetic phenomena at the nanoscale level. From a technological point of view, a wide range of applications is found, for example, in magnetic recording, permanent magnets, ferrofluids, pigments, etc. Pioneering work in this field was done by Stoner and Wohlfarth,[1] by Néel[2] and by Brown.[3] An updated review of the developments in the study of fine magnetic particles can be found in Ref. 4.

For a theoretical investigation of the magnetic behavior of a fine ferromagnetic particle system, it is necessary to make use of simple models. Perhaps the most successful model was developed by Edmund Stoner and Erich Wohlfarth (known as the SW model) more than 50 years ago.[1] In their model it is assumed that the magnetization of a small particle is stable and parallel to the easy magnetic directions when the applied magnetic field is zero. The easy directions are separated by a single energy barrier equal to the product of the particle's volume and anisotropy constant. The magnitude of the magnetization $|\vec{\mu}|$ remains constant during reversible and irreversible changes forced by an external magnetic field. The change in measured magnetization is due to the change of the projection of the magnetization vector along the field direction. With these simple hypotheses a large number of magnetic phenomena in noninteracting systems were explained successfully.

The energy of one of these particles for a given orientation of the uniaxial easy axis $\vec{n}$ in the presence of an external magnetic field $\vec{H}$ consists of two terms,

$$E=E_h+E_a, \tag{1}$$

the first one representing the interaction with the field,

$$E_h=-\vec{\mu}\cdot\vec{H}, \tag{2}$$

and the second one the energy of anisotropy for the uniaxial case,

$$E_a=-KV\left(\frac{\vec{\mu}\cdot\vec{n}}{|\vec{\mu}|}\right)^2, \tag{3}$$

where K is the uniaxial anisotropy constant and V is the particle volume.

For temperatures T close to 0 K, the hysteresis loop of one single-domain uniaxial particle can be calculated by the following process. Starting from a state of very high applied field, when the particle has its magnetization vector parallel to the field, the position of the minimum of the energy is calculated. When the field is decreased the position of this minimum changes continuously and, accordingly, so does the measured magnetization. At some field value two minima appear, instead of one, but only the one closest to the current position of the magnetization is considered, since the energy barrier between the two minima prevents the transition. At a negative field value this energy barrier disappears and a dis-

a)Electronic mail: farivas@usc.es

continuity in the direction of the magnetization occurs. This irreversible jump is the cause of the hysteresis. From this point the energy function again presents only one minimum. The magnetization curve is calculated from the cosine of the angle between the magnetization and field for every field value. By repeating the process for every orientation of the easy axis all possible loops are calculated. Finally, the hysteresis loop of a sample composed of a number of particles oriented along different directions can be calculated by integrating these single loops with the appropriate probability density in the orientation angle. Stoner and Wohlfarth calculated the hysteresis loop for an assembly of uniaxial particles oriented at random. They found $H_c=0.479H_a$ for the coercive field and $M_r=0.5M_s$ for the remanence, where M_s is the saturation magnetization of the material and $H_a=2K/M_s$ is known as the anisotropy field, which is equal to the maximum coercivity possible (shown by the particles if they are oriented along the applied field). The procedure is rigorously valid only at $T=0$ K, since it considers the probability of occupation of other possible states but the energy minimum to be zero.

In contrast to the case of uniaxial anisotropy, the case of cubic magnetocrystalline anisotropy was not treated rigorously until very recently, although materials which present it (such as iron or nickel) are very important in experimental magnetism. Starting from a very high field it was possible to follow the first steps of the hysteresis loop, but after the field had reached the critical value, it was impossible to continue this process because of the existence of several local minima to which the magnetization vector can jump.[5] According to a Néel calculation,[6] for spherical particles with cubic anisotropy oriented at random, the coercive field is $H_c=0.64\,K_1/M_s$, where K_1 is the first anisotropy constant defined below. Although the value seems correct some questions concerning its derivation remain to be resolved.[7,8] The remanence is known, since it was possible to obtain it analytically.[9] The theoretical values are $M_r=0.831M_s$ in the case of $K_1>0$ and $M_r=0.866M_s$ in the case of $K_1<0$.

The first rigorous calculation of the complete hysteresis loop of a set of randomly aligned particles presenting cubic anisotropy was, to our knowledge, presented by Usov and Peschany.[10] In their paper they gave the following upper and lower bounds for the reduced coercivity $h_c=H_c/H_a$ for $T=0$ K: $0.320<h_c<0.335$ when $K_1>0$, and $0.180<h_c<0.200$ when $K_1<0$. They essentially follow the method of Stoner and Wohlfarth; the problem of indetermination of the discontinuous jumps is solved by a dynamical model of evolution, in which there are different probabilities to each adjacent energy minimum.

The purpose of this article is to investigate the hysteresis loops by the Monte Carlo simulation technique (see, e.g., Ref. 11). Beside the possibility of verifying the results discussed above, this method enables us to obtain the complete hysteresis loops, even for cases where the second term of the anisotropy energy is relevant. It has, moreover, the advantage that extensions to nonzero temperature are straightforward. In addition, the method can be used for any kind of distribution of particle orientations and particle sizes.

II. THE MODEL

Since interactions between the particles are neglected, the total energy of the model system is simply the sum of the individual energies of all particles, each one being composed of two parts, the anisotropy energy and the interaction with the external field. For the case of materials with cubic symmetry, the magnetocrystalline anisotropy energy is expressed phenomenologically as a power series of the direction cosines $(\alpha,\beta,\gamma)=(M_x/M,M_y/M,M_z/M)$ of the magnetization in the orthogonal coordinate system formed by the lattice axes. Due to the symmetry of the lattice only those functions which are even in α, β, and γ and symmetric under permutations of these variables have to be considered. The lowest order term, which is of second order, gives no information due to the relation $\alpha^2+\beta^2+\gamma^2=1$ between the direction cosines. The next terms are fourth order terms, either proportional to $\alpha^4+\beta^4+\gamma^4$ or to $\alpha^2\beta^2+\alpha^2\gamma^2+\beta^2\gamma^2$. Both terms can be expressed by each other, since

$$(\alpha^2+\beta^2+\gamma^2)^2=1=(\alpha^4+\beta^4+\gamma^4)+2(\alpha^2\beta^2+\alpha^2\gamma^2+\beta^2\gamma^2), \tag{4}$$

so that it is enough to include only one of them in the series. The next higher term that fulfills the symmetry conditions is $\alpha^2\beta^2\gamma^2$, which is the only one of sixth order. It is customary to include terms up to this sixth order and to write the cubic anisotropy energy as

$$E_a=K_1V(\alpha^2\beta^2+\alpha^2\gamma^2+\beta^2\gamma^2)+K_2V\alpha^2\beta^2\gamma^2, \tag{5}$$

where K_1 and K_2 are the anisotropy constants, whose values are taken from the experiments and usually are sensitive functions of temperature. Higher order terms have never been found necessary to describe experimental observations.

Depending on the sign and relative values of the anisotropy constants the energy topologies will be different. The different easy directions can be summarized as follows:[12] If $K_1>0$ and $K_2>-9K_1$ the easy directions are the crystallographic axes [100]. If $-4/9K_2<K_1<0$ the easy axes are the [110]. For the rest of the cases the easy axes are the body diagonals [111].

Let us consider a particle with cubic anisotropy oriented in an arbitrary position and assume that a magnetic field H is applied along the z axis. If two of the anisotropy axes follow the directions given by $(\theta_1,\phi_1),(\theta_2,\phi_2)$ (the third one is then automatically determined) and the magnetization vector (variable throughout the simulation) is directed towards (θ,ϕ), the direction cosines will be

$$\alpha=\sin\theta_1\sin\theta\cos(\phi_1-\phi)+\cos\theta_1\cos\theta, \tag{6a}$$

$$\beta=\sin\theta_2\sin\theta\cos(\phi_2-\phi)+\cos\theta_2\cos\theta, \tag{6b}$$

$$\gamma^2=1-\alpha^2-\beta^2. \tag{6c}$$

Accordingly, in an applied field the energy of the particle as a function of the orientation of the magnetization is given by

$$E(\theta,\phi)=K_1V(\alpha^2+\beta^2-\alpha^4-\beta^4-\alpha^2\beta^2)+K_2V(\alpha^2\beta^2(1-\alpha^2-\beta^2))-M_sVH\cos\theta. \tag{7}$$

Since we consider only monodispersed particles, and since we want to compare the results with the Stoner-Wohlfarth model, it is convenient to divide both sides by $2|K_1|V$ and use reduced variables for E, H, and M,

$$e(\theta,\phi)=\pm\frac{1}{2}\left(\alpha^2+\beta^2-\alpha^4-\beta^4-\alpha^2\beta^2+\frac{K_2}{K_1}\alpha^2\beta^2(1-\alpha^2-\beta^2)\right)-h\cos\theta, \tag{8}$$

where $h=H/H_a$ with $H_a=2|K_1|/M_s$, and $m=M/M_s$. The plus sign corresponds to the case when K_1 is positive, the minus sign to the case when K_1 is negative.

III. SIMULATION TECHNIQUE

We performed a Monte Carlo (MC) simulation to investigate the hysteresis loops of particles presenting cubic anisotropy. The MC simulation technique is a standard method to study systems with many degrees of freedom. During such a simulation, random numbers are used to simulate statistical fluctuations in order to generate the correct thermodynamical probability distributions.[11] With such a ''computer experiment'' one may obtain information about complex systems which cannot be studied analytically. The purpose of the MC simulation can be either to compare a specific model with real experiments, or to compare its results with analytical theories starting with the same model but using various approximations during analytical treatment. In addition, one is able to obtain microscopic information on the system, which might not be accessible in a real experiment.

A MC simulation always consists of two parts: thermalization and experiment. During the first part, the system is led adiabatically to its thermodynamical equilibrium. This first part is very important, since one starts normally with a nonequilibrium state. After the system is correctly thermalized, we can study its evolution and obtain the properties of interest under the influence of external parameters.

The simulations were performed with a set of 250 randomly orientated particles. Each particle is completely defined by a set of six angles (θ_1,ϕ_1), (θ_2,ϕ_2), and (θ,ϕ), as described above. For each particle, the first easy axis θ_1 is chosen from $[0,\pi]$ with a sinoidal distribution and ϕ_1 is generated from a homogeneous distribution in $[0,2\pi)$. For the second axis we take a perpendicular one $(\theta_1+\pi/2,\phi_1)$ and rotate it with a random angle out of $[0,2\pi)$ in a plane perpendicular to the first axis. These four angles defining the orientation of each particle are kept constant during the simulation. The two remaining angles (θ,ϕ) per particle defining the direction of its magnetization will be variable throughout the MC simulation. Due to the thermalization, their initial values can be chosen arbitrary.

The MC simulation consists of many elementary steps. In every elementary step a particle i is chosen at random and an attempted orientation $\vec{\mu}_{\rm att}^{(i)}$ of the magnetization is generated. The attempted direction is chosen in a spherical segment around the present orientation $\vec{\mu}^{(i)}$, which is used as azimuthal axis, with $\overline{\phi}\in[0,2\pi]$ and $\overline{\theta}\in[0,\delta\theta]$. Then the energy difference Δe between the attempted and the present orientation is calculated. If $\Delta e\leqslant 0$, the magnetization is changed to $\vec{\mu}_{\rm att}^{(i)}$. If $\Delta e>0$, the magnetization is changed with probability $\exp(-\Delta e/t)$ and remains unchanged with probability $1-\exp(-\Delta e/t)$ (Metropolis rates, the random number generator used is the Kirkpatrick-Stoll R250). Here, $t=k_BT/(2|K_1|V)$ is the reduced temperature. In any case the variable counting the elementary steps is increased and the process is continued with the next elementary step. Since our system consists of 250 particles, a complete Monte Carlo step consists of 250 elementary steps, so that in every MC step on average each particle is considered once. Varying the aperture angle $\delta\theta$, i.e., the maximal jump angle, it is possible to modify the range of acceptance to optimize the simulation. Using this kind of local dynamic permits us to detect confinement in metastable states responsible for the hysteresis.[13] Choosing a nonlocal algorithm and drawing the attempted direction independently of the current one, the system would always be superparamagnetic, since it would be possible to explore the whole phase space independently of the temperature. In a compromise between simulations at low and high temperatures we choose $\delta\theta=0.075$. The same value of $\delta\theta$ should be used for simulations at different temperatures, otherwise the direct comparison between obtained loops would not be possible. To perform the complete hysteresis loop a very high field is applied initially at very high temperature. Then the system is carefully thermalized to the desired temperature, in which the total energy of the system is displayed in order to follow the thermalization process and to ensure that the system is thermalized correctly. Since the thermalization is done at very high reduced field $h=10$, in the corresponding equilibrium state almost all moments are aligned with the field, and consequently the system reaches the equilibrium state very fast. Usually about 10000 MC steps are used for thermalization, which is 1–2 orders of magnitude larger than the algorithm's autocorrelation time at zero field. Once the desired temperature is reached, we start the loop by slowly varying the reduced applied field in steps of 0.05 [0.02 if $h\in(-0.5,0.5)$ for better accuracy] in the following way: After changing the field, 2000 MC steps are done, then the magnetization is measured, the field is changed again, and so on. The whole hysteresis loop is repeated for a large number of independent configurations to perform an ensemble average.

IV. THERMAL EVOLUTION OF THE HYSTERESIS LOOPS WITH NEGLIGIBLE K_2

First we consider the case where the higher order anisotropy constant K_2 can be neglected. We obtained hysteresis loops for an ensemble of randomly aligned particles with cubic anisotropy, both for $K_1>0$ and $K_1<0$ [see Figs. 8(a) and 8(d) for sketches of the energy topology). The results are shown in Fig. 1. For $K_1>0$, the reduced remanence $m_r=M_r/M_s$ obtained is $m_r=0.831\pm0.004$. This value is in perfect agreement with the theoretical value.[9] The reduced co-

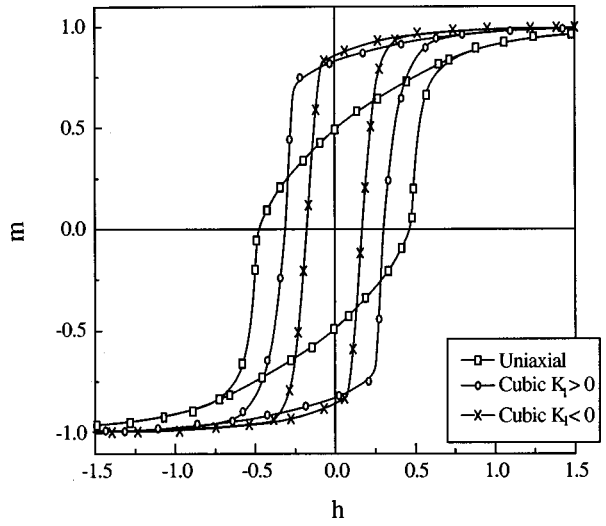

FIG. 1. Reduced hysteresis loops of noninteracting single-domain particles. The particles are randomly oriented in space. For the cubic anisotropy both signs of the anisotropy constant are considered. In addition the loop for the uniaxial case (Stoner-Wohlfarth model) is plotted for comparison. The error bars are smaller than the size of the symbols. The solid lines are splines joining all points obtained, and only a subset of them is shown for clarity.

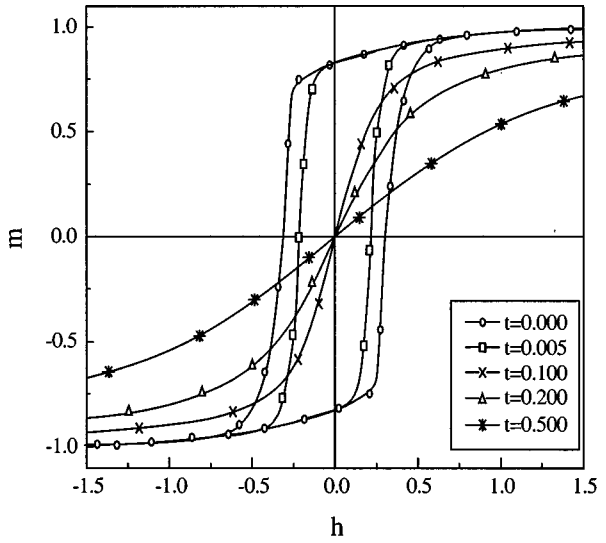

FIG. 2. Temperature evolution of the reduced hysteresis loops of particles presenting cubic anisotropy with $K_1>0$. At high temperatures the loops become superparamagnetic. The error bars are smaller than the size of the symbols, and only a subset of points of the loops obtained is shown for clarity.

ercivity obtained in our simulation is $h_c=0.316\pm0.002$, which is very close to the lower bound given by Usov and Peschany.[10] For $K_1<0$ we obtain $m_r=0.865\pm0.004$ and $h_c=0.183\pm0.002$, the latter being within the bounds given by Usov and Peschany.[10] The error of m_r is given by the statistical error of the point obtained at $h=0$. The reduced coercivity is obtained from a straight line joining the adjacent points, and its error is obtained graphically by joining the same points, taking into account the upper and lower limits given by their error bars.

Next we consider the evolution of the hysteresis loops with temperature. Typical results for $K_1>0$ are shown in Fig. 2. For large temperature, the system approaches the superparamagnetic regime, as can be easily seen in Fig. 2. When performing the same calculations for negative anisotropy constants, we obtain a faster decrease of the reduced coercivity and remanence with temperature. This is easy to understand since particles presenting cubic anisotropy with $K_1>0$ have their six easy directions along the [100], [010], and [001] axes with the minimum energy barrier between them given by $K_1V/4$. In contrast, the anisotropy energy of particles with $K_1<0$ shows eight minima along the body diagonals, and the minimum energy barrier between them is $|K_1|V/12$. This increases the probability of a successful jump over the barrier at a given temperature, and hence implies a faster relaxation. The thermal dependence of the reduced coercive force and remanence is plotted in Fig. 3.

As in real experiments the time interval τ between measuring points plays an important role. A smaller frequency gives the system more time to adapt. At a given temperature τ is no longer long enough for the system to reach thermal equilibrium. This temperature (which depends strongly on τ) is called blocking temperature T_B. All loops shown in the present study were obtained by changing the reduced external field by 0.02 in the sensitive region every 2000 MC steps. This sets the blocking temperature T_B for the case when $K_1>0$ around $k_BT_B/(2K_1V)=0.05$ in reduced units. To avoid this dependence on the measuring time, a rescaling of the temperature by dividing it by the blocking temperature can be carried out. In any case, the functional dependence of the magnetic parameters will be the same, as will the shape of the loops.

It should also be kept in mind that the parameters which enter into the definition of the reduced magnitudes, like M_s and the anisotropy constants, depend strongly on tempera-

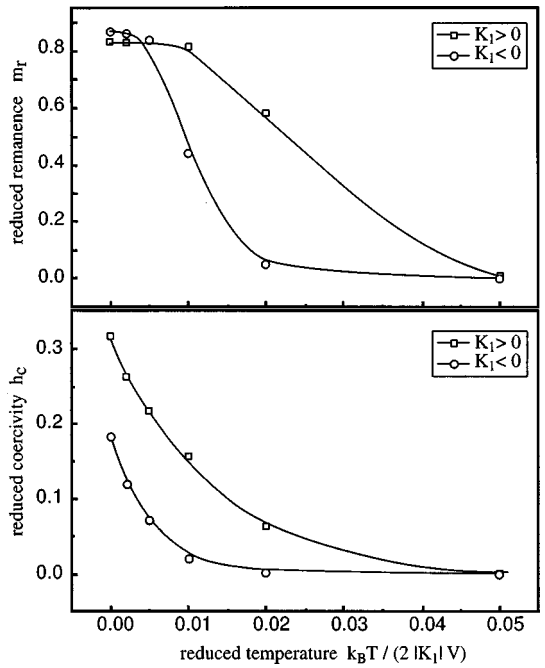

FIG. 3. Temperature dependence of the reduced coercivity and remanence. Both signs of the first constant of cubic anisotropy are considered.

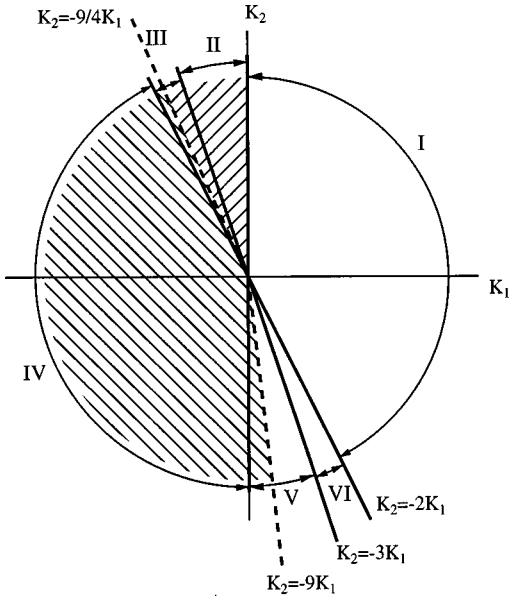

FIG. 4. Influence of the relative values of the cubic anisotropy constants on the anisotropy energy. In the unshaded region the easy axes are along [100], in the region shaded lower left to upper right the easy axes are along [110], and in the region shaded upper left to lower right the easy axes are along [111]. Also shown are the six different regions where the main directions show local maxima or minima changing the energy topology (see Table I).

ture. Hence, the remanence and coercivity may depend differently on temperature as the reduced remanence and coercivity shown in Fig. 3 do.

V. INFLUENCE OF THE SECOND ANISOTROPY CONSTANT

By using the same Monte Carlo approach it is possible to investigate more complicated cases that are not accessible analytically, such as the effect of the second anisotropy constant K_2. In order to explain the experimental results for bulk materials, it is often not necessary to include this second term, but it is known to be very important in other cases such as in materials with reduced dimensionality. As happens with K_1, K_2 can also take positive or negative values and can even change signs depending on temperature. We performed simulations to study whether the sign and ratio $R \equiv K_2/K_1$ of the second and first anisotropy constants have a significant influence on the reduced hysteresis loops.

The effect of the relative variation of K_2 with respect to K_1 is summarized in Fig. 4. The position of the easy axes as a function of both anisotropy constants, as discussed before, are represented by the shaded areas. In addition, the topology

TABLE I. Local minima and maxima for cubic anisotropy energy.

Region	[100]	[110]	[111]
I	minimum		maximum
II	maximum	minimum	maximum
III	maximum	minimum	minimum
IV	maximum		minimum
V	minimum	maximum	minimum
VI	minimum	maximum	maximum

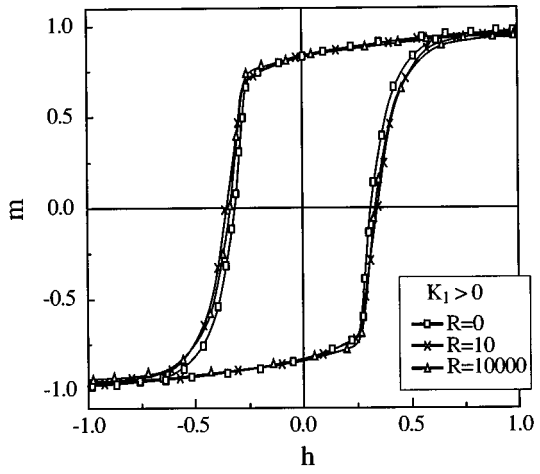

FIG. 5. Influence of the second anisotropy constant on the reduced hysteresis loops of randomly aligned particles at $T=0$ K, where $K_1>0$ and $K_2>0$. R indicates the ratio K_2/K_1. The error bars are smaller than the size of the symbols, and a subset of some points of the loops obtained is shown for clarity.

of the cubic anisotropy energy is shown. There are six regions, which are represented in Fig. 4 by roman numerals. The different regions correspond to the relative values of the anisotropy constants which change the directions of the local minima or maxima of the anisotropy energy function. A summary of the different possibilities is given in Table I. The different energy topologies are sketched in Fig. 8.

If both K_1 and K_2 are positive, the topology of the energy is barely modified from the case of negligible K_2. The hysteresis loop does not noticeably change, even for values of K_2 much higher than the values reported in the literature; examples are presented in Fig. 5. If $K_1>0$ and $K_2<0$ the energy landscape is more sensitive to their ratio R, but the overall effect of K_2 on the global hysteresis loop is still small. In Fig. 6 some loops are shown for different ratios R

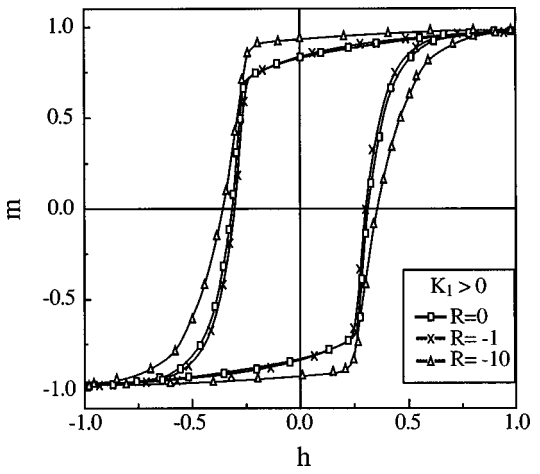

FIG. 6. Influence of the second anisotropy constant on the reduced hysteresis loops of randomly aligned particles at $T=0$ K, where $K_1>0$ and $K_2<0$. R indicates the ratio K_2/K_1. The error bars are smaller than the size of the symbols, and a subset of some points of the loops obtained is shown for clarity.

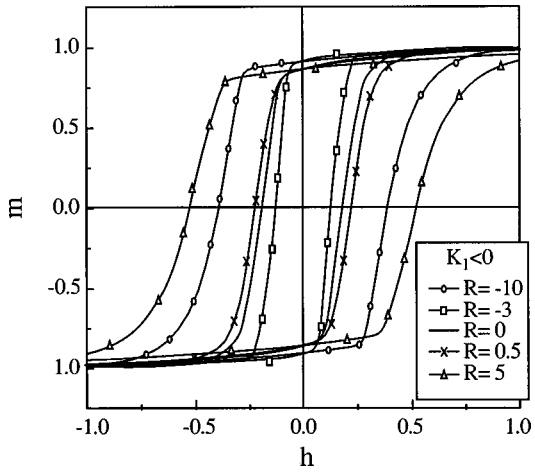

FIG. 7. Influence of the second anisotropy constant on the reduced hysteresis loops of randomly aligned particles at $T=0$ K, where $K_1<0$ and K_2 can be positive or negative. R indicates the ratio K_2/K_1. The error bars are smaller than the size of the symbols, and only a subset of points of the loops obtained is shown for clarity.

between the first and second anisotropy constants. The reduced remanence changes for $R<-3$ are due to the change in topology.

This picture changes when K_1 is negative. In this case, the energy surface is more sensitive to the value of K_2, which is reflected by the fact that reduced remanence and coercivity can suffer conspicuous changes. Several values for R are considered for the numerical simulation, although the real values rarely exceed unity. For $R\in(-2,\infty)$ the reduced remanence remains unchanged since the energy topology does not change significantly. With increasing R, the reduced coercivity increases continuously. With $R\in(-3,-2)$ the topology changes, resulting in a discontinuity in the reduced remanence and a reduced coercivity that increases with the increasing absolute value of the ratio. In Fig. 7 some of the loops are presented. As it can be seen for values of R about 0.5 (which can be found in real materials) the loops undergo an obvious change.

VI. CONCLUSIONS

We obtained the complete hysteresis loops for noninteracting single-domain particles with cubic anisotropy for both signs of the first and second anisotropy constants. In the case $K_2=0$, our numerical results agree well with the previous published results for reduced remanence and complete loops obtained by Usov and Peschany. The second term of the cubic anisotropy energy expansion is of importance when the first anisotropy constant is negative. The local dynamic used in our algorithms also allow us to study the influence of temperature on the hysteresis loops, hence it is possible to obtain the thermal dependence of important magnetic parameters such us coercivity or remanence. Additionally, at high temperature, superparamagnetic curves can be obtained.

The simple model studied does not take into account interparticle interactions, but it may be of interest in the case of very diluted systems of single-domain particles. The influence of dipolar interactions will be our next objective.

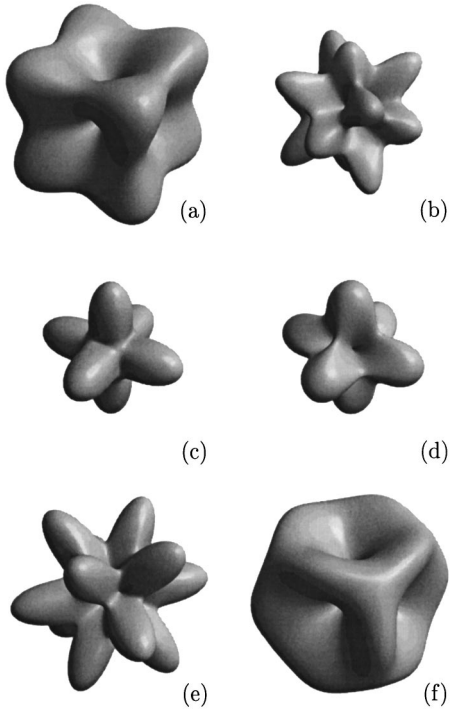

FIG. 8. Magnetocrystalline anisotropy energy for particles with cubic symmetry. Cases where (a) $K_1>0$ and $K_2>-2K_1$ (i.e., region I, $R=K_2/K_1=0$ was used for the plot), (b) $K_1<0$ and $K_2>-3K_1$ (i.e., region II, $R=-10$ is used), (c) $K_1<0$ and $-2K_1<K_2<-3K_1$ (i.e., region III, $R=-5/2$ is used), (d) $K_1<0$ and $K_2<-2K_1$ (i.e., region IV, $R=6$ is used), (e) $K_1>0$ and $K_2<-3K_1$ (i.e., region V, $R=-7$ is used), and (f) $K_1>0$ and $-3K_1<K_2<-2K_1$ (i.e., region VI, $R=-5/2$ is used).

ACKNOWLEDGMENTS

We acknowledge partial support of ''Act. Integrada Hispano-Alemana HA98-136'' (Germany, Spain) and project Ref. 1FD97-0148 (MAT), Ministerio de Educación y Cultura (Spain). One author (J.G.-O.) wishes to thank the autonomical government of Galicia (Xunta de Galicia) for its financial help. A second author (M.P.) would like to thank the Deutsche Forschungsgemeinschaft for financial support.

[1] E. C. Stoner and E. P. Wohlfarth, Philos. Trans. R. Soc. London, Ser. A **240**, 599 (1948); reprinted in IEEE Trans. Magn. **27**, 3475 (1991).
[2] L. Néel, Ann. Geophys. (C.N.R.S.) **5**, 99 (1949).
[3] W. F. Brown, Phys. Rev. **130**, 1677 (1963).
[4] J. L. Dormann, D. Fiorani, and E. Tronc, Adv. Chem. Phys. **98**, 283 (1997).
[5] E. W. Lee and J. E. L. Bishop, Proc. Phys. Soc. London **89**, 661 (1966).
[6] L. Néel, C.R. Acad. Sci. (Paris) **224**, 1488 (1947).
[7] C. E. Johnson and W. F. Brown, J. Appl. Phys. **32**, 2435 (1961).
[8] A. H. Morrish, *The Physical Principles of Magnetism* (Wiley, New York, 1965), p. 351.
[9] R. Gans, Ann. Phys. (Leipzig) **15**, 28 (1932).
[10] N. A. Usov and S. E. Peschany, J. Magn. Magn. Mater. **174**, 247 (1997).
[11] K. Binder and D. W. Heermann, *Monte Carlo Simulations in Stastical Physics*, Springer Series in Solid State Science, Vol. 80, 2nd ed. (Springer, Berlin, 1992).
[12] R. M. Bozorth, *Ferromagnetism* (IEEE, New York, 1993), Chap. 12.
[13] D. A. Dimitrov and G. M. Wysin, Phys. Rev. B **54**, 9237 (1996).